Revised Version
Revised parts were yellow-highlighted.

Structure and dissolution behavior of orthophosphate MgO–CaO–P_2O_5–Nb_2O_5 glass and glass-ceramic

Sungho Lee, Anthony L. B. Maçon, Toshihiro Kasuga*

Department of Frontier Materials, Graduate School of Engineering

Nagoya Institute of Technology, Gokiso-cho, Showa-ku, Nagoya 466-8555, Japan

* Corresponding author *E-mail address*: kasuga.toshihiro@nitech.ac.jp

Abstract

The aim of this work is to investigate the effect of lowering the phosphate content, from 27 to 20 mol%, in calcium-phosphate invert glass/glass-ceramic containing magnesia and niobia ($MgO\text{-}CaO\text{-}P_2O_5\text{-}Nb_2O_5$) on the structure and dissolution properties. According to ^{31}P solid-state nuclear magnetic resonance (NMR) and Raman spectroscopies, glass containing 20 mol% of P_2O_5 was exclusively composed of orthophosphate (Q_P^0), whereas orthophosphate and pyrophosphate (Q_P^1) coexisted in 27 mol% P_2O_5 glass. Tetrahedral niobate was detected by Raman spectroscopy with 20 mol% phosphate, suggesting that niobate acts as a network former and therefore cross-links orthophosphate groups together (P-O-Nb bonds). The equivalent glass-ceramic consisted of crystalline phases (β-$Ca_3(PO_4)_2$, $Mg_3(PO_4)_2$ and $Mg_3Ca_3(PO_4)_4$), which did not contain niobate, and a residual glassy phase. The glass with 20 mol% P_2O_5 showed a lower chemical durability than the glass with 27 mol% P_2O_5, which was likely due to the formation of P-O-Mg bonds, which favor hydrolysis. The glass-ceramic chemical durability was improved after crystallization, probably because of an increase in the niobate concentration of the residual glassy phase.

Highlights

- A glass based on a network consisting of orthophosphate group was prepared.
- Niobate tetrahedra and magnesium crosslink orthophosphate groups in the glass.
- The glass-ceramic included orthophosphate crystal phases.

Keywords

Biomaterials, phosphate invert glass, orthophosphate, magnesium, niobium, structure

1. Introduction

Calcium phosphate invert glasses consist of short phosphate groups such as ortho- and pyrophosphates (*i.e.*, Q_p^0 and Q_p^1, respectively); they are excellent candidates for bioactive coatings on bioinert implants because of their controlled degradation and affinity to titanium, especially when they contain titania or niobia [1,2]: $60CaO{\cdot}30P_2O_5{\cdot}(10-x)Na_2O{\cdot}xTiO_2/Nb_2O_5$ (mol%, x = 0 ~ 10, denoted by PIG-Ti/Nb). TiO_2 or Nb_2O_5 improve their glass-forming ability and chemical durability [3,4] by forming P-O-Ti/Nb bonds, crosslinking the phosphate groups [5,6]. A Ti–29Nb–13Ta–4.6Zr (TNTZ) alloy was successfully coated with PIG-Ti by heat treatment at 800°C for 1 h; the resulting layer included β-$Ca_3(PO_4)_2$, β-$Ca_2P_2O_7$, and TiO_2 (rutile) crystal phases, which exhibited a strong affinity for TNTZ [7,8]. The coated alloy showed good bioactivity *in vivo* [9]. However, PIG-Nb stimulates alkaline phosphatase activity (ALP), which is a marker for differentiation of osteoblast-like cells, with a trace amount of Nb^{5+} ions dissolved from the glasses (0.04 ~ 0.06 mM) [10].

In our previous work, MgO-CaO-P_2O_5-Nb_2O_5 invert glasses consisting of Q_p^0 and Q_p^1 groups with various MgO/CaO ratios were prepared to increase in bioactivity of PIG-Nb by incorporating MgO in the glass structure [11]. Magnesium is an important element for bone regeneration as a slight variation in its concentration *in vivo* influences

bone strength [12] and promotes cell adhesion [13], proliferation [14], and differentiation [15]. Mg^{2+} ions in phosphate glasses act as an intermediate oxide, *i.e.*, a network modifier and/or former [16,17]. In our previous work [11], a glass with the nominal composition of $33.75MgO·33.75CaO·27P_2O_5·5.5Nb_2O_5$ in mol% (denoted by 27P) showed high chemical durability, *e.g.*, the dissolution rate was approximately 5% at day 7, with magnesium being successfully released from the glass.

In this work, we aim to improve the dissolution ability of $MgO-CaO-P_2O_5-Nb_2O_5$ glass and the equivalent glass-ceramic by increasing the (Mg + Ca)/P ratio from 1.25 to 1.875, meaning that the phosphate content decreases from 27 mol% to 20 mol%. The structure and dissolution behaviors of the glass and the glass-ceramic were examined towards the design of a new bioactive coating.

2. Material and methods

$37.5MgO·37.5CaO·20P_2O_5·5Nb_2O_5$ (mol%, denoted by 20P) and $33.75MgO·33.75CaO·27P_2O_5·5.5Nb_2O_5$ (mol%, denoted by 27P) glasses were obtained by melt-quenching. Glass batches were prepared by manually mixing MgO (99.0%), $CaCO_3$ (99.5%), H_3PO_4 (85% liquid), and Nb_2O_5 (99.9%), which was subsequently dried under an infrared lamp overnight and then stored at 140°C. All the reagents were

purchased from Kishida Chemical Co., Japan. After melting in a platinum crucible at 1500°C for 30 min, the melt was quenched by splatting between two stainless-steel plates. The composition of 20P was determined by energy-dispersive X-ray spectroscopy and given as an average of three samples (EDX, JED-2300, JEOL). A glass-ceramic of 20P was prepared by heating at 750°C for 3 h (denoted by 20P-GC). Crystalline phases were analyzed by powder X-ray diffraction (XRD, X'pert-MPD, PANalytical), and the cross-section (mirror-polished) of the glass-ceramic was observed by scanning electron microscopy (SEM, JSM-6301F, JEOL). The glass transition (T_g) and crystallization temperatures (T_c, defined as the onset of crystallization) of 20P were determined from differential thermal analysis (DTA; heating rate: 5 K/min, Thermoplus TG8120, Rigaku). The glass structure was investigated by laser Raman spectroscopy, focusing on the spectral range from 220 to 1300 cm^{-1} (NRS-3300, 532.08 nm, 6.4 mW, JASCO) and solid-state ^{31}P magic angle spinning nuclear magnetic resonance (MAS-NMR, JNM-ECA600II, JEOL), 242.955 MHz in a 3.2-mm rotor spinning at 15 kHz. Single-pulse experiments were conducted using 0.1-μs pulses (256 in total) spaced by 5 s using ammonium dihydrogen phosphate as a reference (1.0 ppm); the spectra were reconstructed with a Gaussian fit.

Glass powders were obtained by grinding and sieving, yielding particles between

125 and 250 μm. Dissolution tests were carried out by immersing 15 mg of the samples in 15 mL of glass powder in 50 mM Tris buffer solution (TBS) at 37°C and 7.4 pH over 7 days. The concentration profiles of Mg^{2+}, Ca^{2+}, P^{5+}, and Nb^{5+} ions in TBS were measured by inductively coupled plasma atomic emission spectroscopy (ICP-AES, ICPS-7510, Shimadzu). The molar dissolution fraction of the different elements were calculated using the following equation [18]:

$$Dissolution\ rate\ (\%) = \frac{(a/M_{wa})\times 10^5}{(Frac_{,a}\times M_{w,glass})/(m_{glass}\times V_{solution})} \quad (1)$$

where a is the concentration of the element of interest in $mg.L^{-1}$; M_{wa} is the atomic weight of the ion; $Frac_{,a}$ is the nominal molar fraction of the element in the glass; and $M_{w,glass}$, m_{glass}, and $V_{solution}$ are the molecular weight, the mass of the sample soaked, and the volume of TBS, respectively.

3. Results

The compositions of 20P and 27P were measured by EDX and are given in mol%: (34.2 ± 2.0)MgO·(39.4 ± 2.1)CaO·(21.3 ± 0.2)P_2O_5·(5.1 ± 0.2)Nb_2O_5, and (35.4 ± 0.2)MgO·(29.7 ± 0.2)CaO·(27.7 ± 0.1)P_2O_5·(7.2 ± 0.1)Nb_2O_5, respectively. A slight variation was observed from the nominal composition, which could be explained by magnesium being a relatively light element and the overlap in the signals given by

phosphorus $K\alpha$ (2.013 eV) and niobium $L\alpha$ (2.166 eV). The DTA curve (Supplementary Fig. S1) showed that the T_c of 20P was 717°C, and, below T_c, 20P exhibited three T_g values, which were 670°C (T_{g_3}), 640°C (T_{g_2}), and 603°C (T_{g_1}). The T_c and T_g values of 27P were 732°C and 633°C, respectively. 20P and 27P showed no significant difference in glass forming ability compared with PIG-Ti/Nb because magnesium in 20P and 27P forms P-O-Mg bonds and increases the ability[16].

Structural investigation of the glass was performed with Raman spectroscopy and ^{31}P MAS-NMR. Figure 1 shows that the vibrations corresponding to orthophosphate (Q_p^0) and pyrophosphate (Q_p^1) could be observed from 27P, whereas 20P only exhibited the spectral signature of orthophosphate (Q_p^0) as follows [17,19,20]: the P-O stretching mode of the Q_p^1 chain terminator at 1130 cm^{-1}, the $(PO_3)_{sym}$ stretching vibrations of the non-bridging oxygen in Q_p^1 at 1040 cm^{-1}, the $(PO_4)_{sym}$ stretching mode of the non-bridging oxygen in Q_p^0 at 965 cm^{-1}, the P-O-P$_{sym}$ stretching mode of the bridging oxygen in Q_p^1 at 755 cm^{-1}, the symmetric stretching of the P-O bonds of the Q_p^0 at 590 cm^{-1}, the symmetric stretching of the O-P-O bending modes of the Q_p^0 at 430 cm^{-1}, and the bending mode of phosphate chains with cation modifier at 250–350 cm^{-1}. Similarly, the coordination of niobate differed between 27P and 20P. In 27P, vibrations at 905 cm^{-1} and 650 cm^{-1} corresponding to isolated units and cross-linked octahedron units (NbO_6) [4],

respectively, as well as vibrations at 840 cm^{-1} corresponding to NbO_4 tetrahedral groups [4] were observed, whereas 20P was solely composed of NbO_4 tetrahedral units. ^{31}P MAS-NMR spectra corroborated the result obtained by Raman spectroscopy with Q_p^0 and Q_p^1 groups detected for 27P and only Q_p^0 for 20P (Fig. 1 inset).

Glass-ceramic derived from 20P, namely 20P-GC, was obtained by heating, and the crystallization was monitored by XRD, as shown in Fig. 2. The 20P sample exhibited a broad halo-peak, whereas 20P-GC displayed sharp peaks corresponding to β-$Ca_3(PO_4)_2$ (ICDD card: 70-2065), $Mg_3(PO_4)_2$ (ICDD card: 75-1491), and $Mg_3Ca_3(PO_4)_4$ (ICDD card: 73-1182). The inset in Fig. 2 shows an SEM image of the cross-section surface of 20P-GC, confirming the coexistence of a crystal phase (bright) and a residual glassy phase (dark).

The dissolution behaviors of 27P, 20P, and 20P-GC were evaluated by immersion in Tris buffer solution (TBS). Figures 3 shows the ion-released percentages of magnesium, phosphorus, calcium, and niobium from the samples. Congruent dissolution was observed from 27P, whereas 20P and 20P-GC showed inhomogeneous dissolution behavior. For instance, the molar fraction of phosphorus in solution from 20P at day 7 was 21%, which is twice those of magnesium and calcium. SEM observation of the surface of the 20P after 7 d of soaking suggested that a gel-like layer of niobium, phosphorus, magnesium, and

calcium formed on the surface of glass. The proportion of ions in solution at any given time point was lower for 20P-GC than 20P.

4. Discussion

The glassification degree of 20P was 0.13, which was calculated using ($T_c - T_{g\_1}$) / T_{g_1} [21]. This value is higher than those for PIG-Ti (0.08) [22], PIG-Nb (0.09) [2], and 27P (0.11) [11], which indicates a better glass forming ability. The 20P showed three T_g values, which may indicate the coexistence of several network structures where niobate [4,5] and magnesium [16,17] act as network formers. In 20P, phosphate and niobate were present as isolated orthophosphate (Q_p^0) and tetrahedral NbO_4. In our previous work, niobates in $(94.5 - y)MgO/CaO \cdot yP_2O_5 \cdot 5.5Nb_2O_5$ glass (mol%, $y = 63 - 69$), with the mix of their octahedron and tetrahedron units, acted as a network former and an intermediate oxide [18,22]. It is likely that, with the decrease in phosphate content in 20P, niobate acted solely as a network former, which explains the presence of only tetrahedral NbO_4 [4,6]. This would also imply that P-O-Nb bonds formed [4,6]. Similar remarks can be made for magnesium, which can also act as a network former and create P-O-Mg bonds [16,17]. Thus, the cumulative network forming ability of niobate and magnesium at low phosphate content, such as in 20P, could explain the presence of only orthophosphate groups (Q_p^0).

The resulting glass-ceramic consisted of crystalline phases, which contained only Q_p^0 groups.

A noticeable decrease in the chemical durability was observed when the phosphate content of 27P was decreased, which was due to the increase in the content of P-O-Mg bonds in 20P [18]. P-O-Mg bonds are similar to Si-O-Mg bonds and weaken the glass network structure [23] and the resistance to hydrolysis [24]. In our previous work, the chemical durability of phosphate invert glasses containing intermediate oxide (e.g. TiO_2 or Nb_2O_5) decreased with increasing MgO content in the glasses [11,18,25]. Because of the lower chemical durability of 20P, a gel-like layer on the glass surface was observed after soaking in TBS. The chemical durability of 20P could be improved by heating, yielding 20P-GC, because of the less soluble crystalline phases. The residual glassy phase was considered to contain a greater amount of niobate than 20P, since niobate was not present in any of the crystalline phases of 20P-GC. Thus, it is likely that niobate improved the chemical durability of the residual glass phase.

20P-GC has great potential as a bioactive coating on titanium or its alloys. The glass-ceramic includes β-$Ca_3(PO_4)_2$, which is a well-known bone implant [26], and can release magnesium, which can stimulate bone regeneration [27,28]. In addition, a trace amount of niobium released from the residual glassy phase is expected to enhance the

differentiation of osteoblast-like cells [10].

5. Conclusions

In this work, we showed that decreasing the amount of P_2O_5 in MgO-CaO-P_2O_5-Nb_2O_5 phosphate invert glass greatly influenced the network structure. With 20 mol% of P_2O_5, phosphate was only present as orthophosphate, crosslinked by tetrahedral niobate (NbO_4) and magnesium. The glass-ceramic equivalent showed orthophosphate crystal phases, such as β-$Ca_3(PO_4)_2$, $Mg_3(PO_4)_2$, and $Mg_3Ca_3(PO_4)_4$, which improved the chemical durability of the glass.

Acknowledgements

This work was supported in part by JSPS KAKENHI Grant Numbers 26289238 and 267992.

References

[1] T. Kasuga, Y. Abe, Calcium phosphate invert glasses with soda and titania, *J. Non-Cryst. Solids* 243 (1999) 70–74.

[2] H. Maeda, S. Lee, T. Miyajima, A. Obata, K. Ueda, T. Narushima, T. Kasuga, Structure and physicochemical properties of CaO-P_2O_5-Nb_2O_5-Na_2O glasses, *J. Non-Cryst. Solids* 432 (2016) 60–64.

[3] A. Kishioka, M. Haba, M. Amagasa, Glass formation in multicomponent phosphate systems containing TiO_2, *Bull. Chem. Soc. Jpn.* 47 (1974) 2493–2496.

[4] S. M. Hsu, J. J. Wu, S. W. Yung, T. S. Chin, T. Zhang, Y. M. Lee, C. M. Chu, J. Y. Ding, Evaluation of chemical durability, thermal properties and structure characteristics of Nb–Sr–phosphate glasses by Raman and NMR spectroscopy, *J. Non-Cryst. Solids* 358 (2012) 14–19.

[5] R. K. Brow, D. R. Tallant, W. L. Warren, A. McIntyre, D. E. Day, Spectroscopic studies of the structure of titanophosphate and calcium titanophosphate glasses, *Phys. Chem. Glasses* 38 (1997) 300–306.

[6] C. M. Chu, J. J. Wu, S. W. Yung, T. S. Chin, T. Zhang, F. B. Wu, Optical and structural properties of Sr–Nb–phosphate glasses, *J. Non-Cryst. Solids* 357 (2011) 939–945.

[7] T. Kasuga, M. Nogami, M. Niinomi, T. Hattori, Bioactive calcium phosphate invert glass-ceramic coating on *β*-type Ti–29Nb–13Ta–4.6Zr alloy, *Biomaterials* 24 (2003) 283–290.

[8] T. Kasuga, M. Nogami, M. Niinomi, Joining of calcium phosphate invert glass-ceramics on a *β*-type titanium alloy, *J. Am. Ceram. Soc.* 86 (2003) 1031–1033.

[9] T. Kasuga, T. Hattori, M. Niinomi, Phosphate glasses and glass-ceramics for biomedical applications, *Phosphorus Res. Bull.* 26 (2012) 8–15.

[10] A. Obata, Y. Takahashi, T. Miyajima, K. Ueda, T. Narushima, T. Kasuga, Effects of niobium ions released from calcium phosphate invert glasses containing Nb_2O_5 on osteoblast-like cell functions, *ACS Appl. Mater. Interfaces* 4 (2012) 5684–5890.

[11] S. Lee, H. Maeda, A. Obata, K. Ueda, T. Narushima, T. Kasuga, Structures and dissolution behaviors of MgO–CaO–P_2O_5–Nb_2O_5 glasses, *J. Non-Cryst. Solids* 438 (2016) 18-25.

[12] T. Okuma, Magnesium and bone strength, *Nutrition* 17 (2001) 679–680.

[13] M. Takeichi, T. S. Okada, Roles of magnesium and calcium ions in cell-to-substrate adhesion, *Exp. Cell Res.* 74 (1972) 51–60.

[14] F. I. Wolf, A. Cittadini, Magnesium in cell proliferation and differentiation, *Front. iosci*. 4 (1999) d607–d617.

[15] A. Saboori, M. Rabiee, F. Moztarzadeh, M. Sheikhi, M. Tahriri, M. Karimi, Synthesis, characterization and in vitro bioactivity of sol-gel-derived SiO_2-CaO-P_2O_5-MgO bioglass, *Mater. Sci. Eng. C* 29 (2009) 335–340.

[16] F. Fayon, D. Massiot, K. Suzuya, D. L. Price, ^{31}P NMR study of magnesium phosphate glasses, *J. Non-Cryst. Solids* 283 (2001) 88–94.

[17] M. A. Karakassides, A. Saranti, I. Koutselas, Preparation and structural study of binary phosphate glasses with high calcium and/or magnesium content, *J. Non-Cryst. Solids* 347 (2004) 69–79.

[18] S. Lee, H. Maeda, A. Obata, K. Ueda, T. Narushima, T. Kasuga, Structures and dissolution behaviors of MgO-P_2O_5-TiO_2/Nb_2O_5 (Mg/P ≥ 1) invert glasses, *J. Ceram. Soc. Jpn.* 123 (2015) 942–948.

[19] R. K. Brow, D. R. Tallant, S. T. Myers, C. C. Phifer, The short-range structure of zinc polyphosphate glass, *J. Non-Cryst. Solids* 191 (1995) 45–55.

[20] A. Moguš-Milanković, A. Gajović, A. Šantić, D. E. Day, Structure of sodium phosphate glasses containing Al_2O_3 and/or Fe_2O_3. Part I, *J. Non-Cryst. Solids* 289 (2001) 204–213.

[21] M. Ouchetto, B. Elouadi, S. Parke, Study of lanthanide zinc phosphate glasses by differential thermal analysis, *Phys. Chem. Glasses* 32 (1991) 22–28.

[22] S. Lee, H. Maeda, A. Obata, K. Ueda, T. Narushima, T. Kasuga, Structures and dissolution behaviors of $CaO–P_2O_5–TiO_2/Nb_2O_5$ (Ca/P ≥ 1) invert glasses, *J. Non-Cryst. Solids* 426 (2015) 35–42.

[23] S. J. Watts, R. G. Hill, M. D. O'Donnell, R. V. Law, Influence of magnesia on the structure and properties of bioactive glasses, *J. Non-Cryst. Solids* 356 (2010) 517–524.

[24] D. S. Brauer, N. Karpukhina, G. Kedia, A. Bhat, R. V. Law, I. Radecka, R. G. Hill, Bactericidal strontium-releasing injectable bone cements based on bioactive glasses, *J. Royal Soc. Interface* 10 (2012) 20120647.

[25] H. Morikawa, S. Lee, T. Kasuga, D.S. Brauer, Effects of magnesium for calcium substitution in $P_2O_5–CaO–TiO_2$ glasses, *J. Non-Cryst. Solids* 380 (2013) 53–59.

[26] C. P. A. T. Klein, K. de Groot, A. A. Drissen, H. B. M. van der Lubbe, Interaction of biodegradable β-whitlockite ceramics with bone tissue: An in vivo study, *Biomaterials* 6 (1985) 189–192.

[27] M. Diba, F. Tapia, A. R. Boccaccini, L. A. Strobel, Magnesium-Containing Bioactive Glasses for Biomedical Applications, *Int. J. Appl. Glass Sci.* 3 (2012) 221–253.

[28] A. Hoppe, N. S. Güldal, A. R. Boccaccini, A review of the biological response to ionic dissolution products from bioactive glasses and glass-ceramics, *Biomaterials* 32 (2011) 2757–2774.

Figure captions

Figure 1: (A) Laser Raman spectra and (B) ^{31}P MAS-NMR spectra of the 20P and 27P.

Figure 2: XRD patterns of 20P and 20P-GC. Inset shows the SEM image of the cross-section surface of 20P-GC.

Figure 3: Released ions amount in TBS from 27P, 20P and 20P-GC. The error bars represent the standard deviation. The inset showed SEM images of 20P surface after being soaked in TBS for 7 days.

Figures

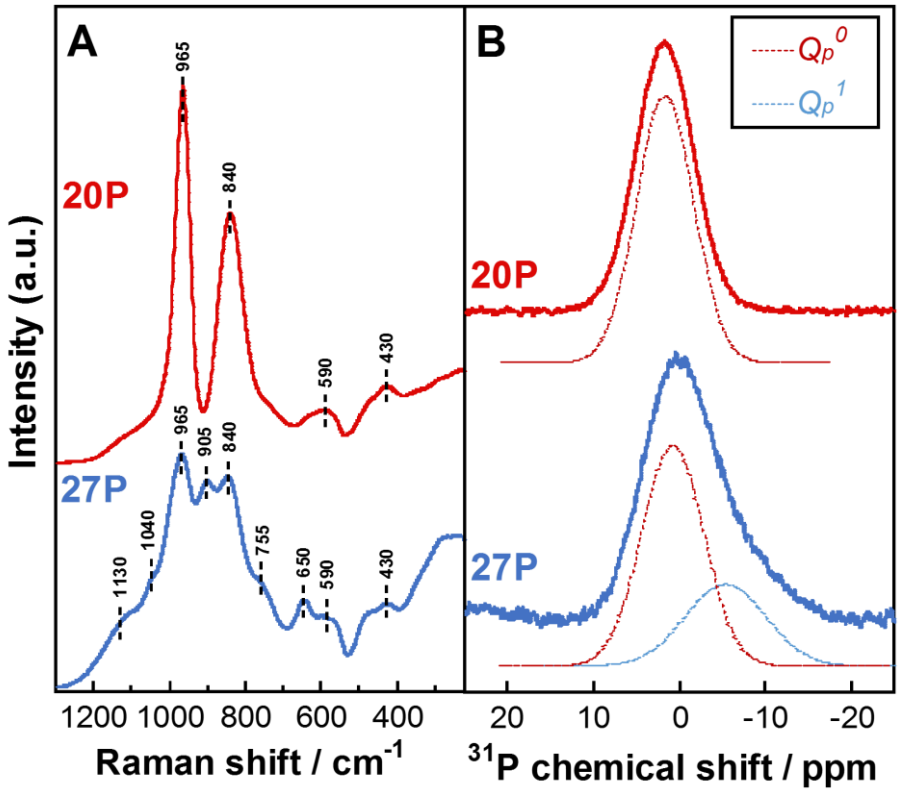

Fig. 1

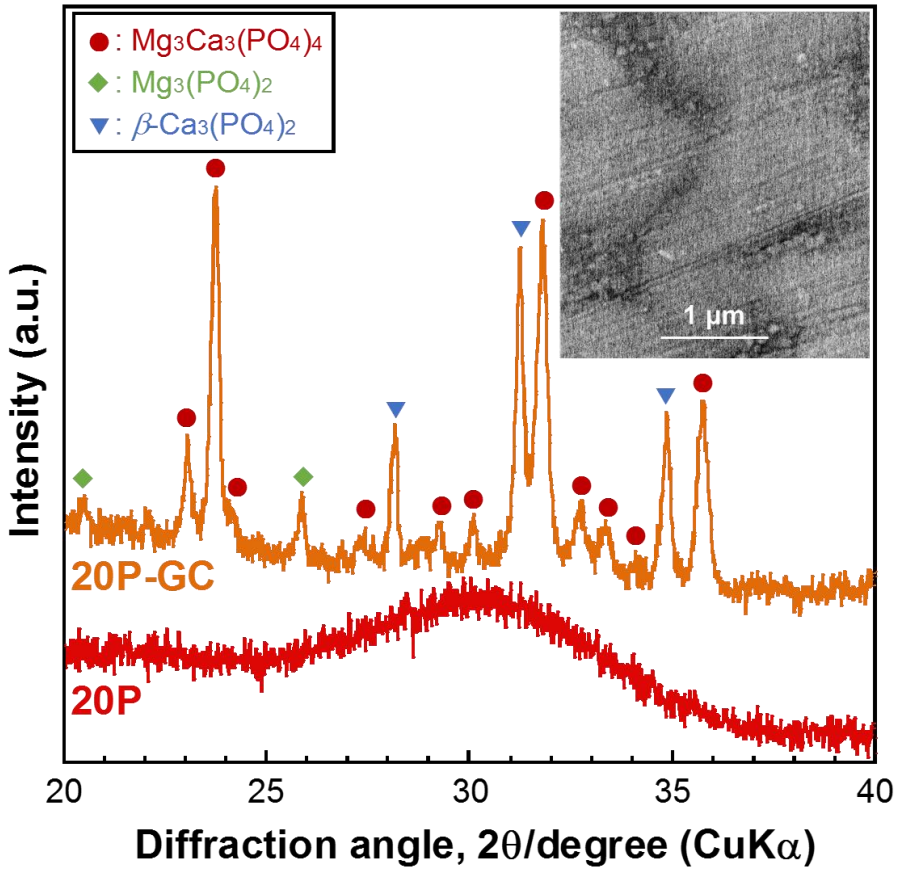
● : Mg3Ca3(PO4)4
◆ : Mg3(PO4)2
▼ : β-Ca3(PO4)2
1 μm
20P-GC
20P
Intensity (a.u.)
20
25
30
35
40
Diffraction angle, 2θ/degree (CuKα)

Fig. 2

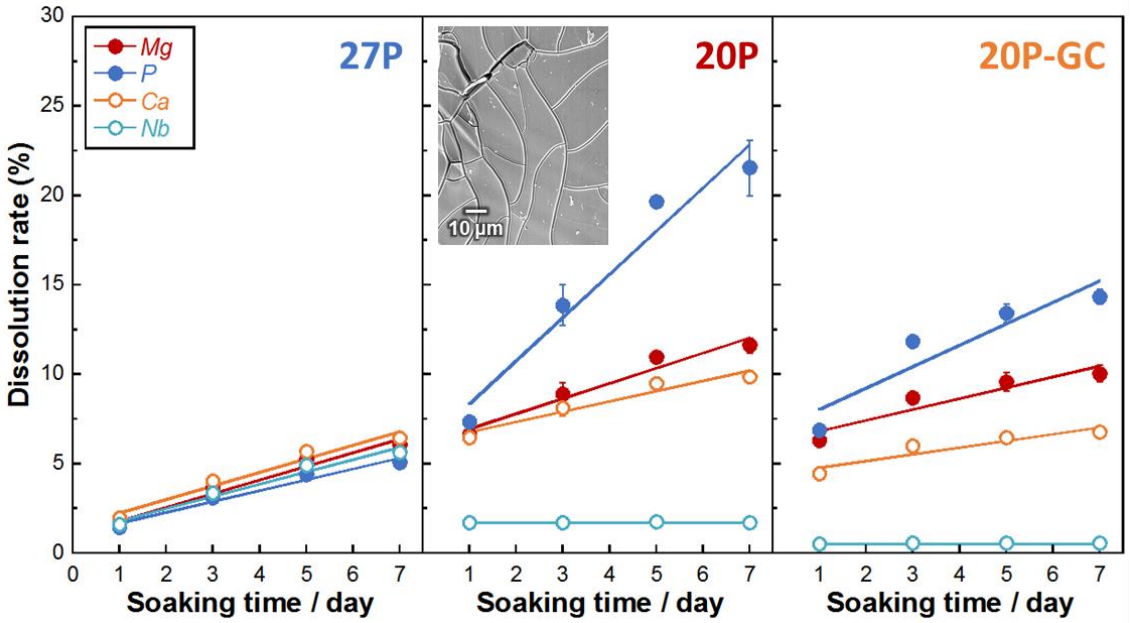
Mg
P
Ca
Nb
27P
20P
20P-GC
10 μm
Dissolution rate (%)
Soaking time / day
Soaking time / day
Soaking time / day

Fig. 3

Supplementary Figure S1

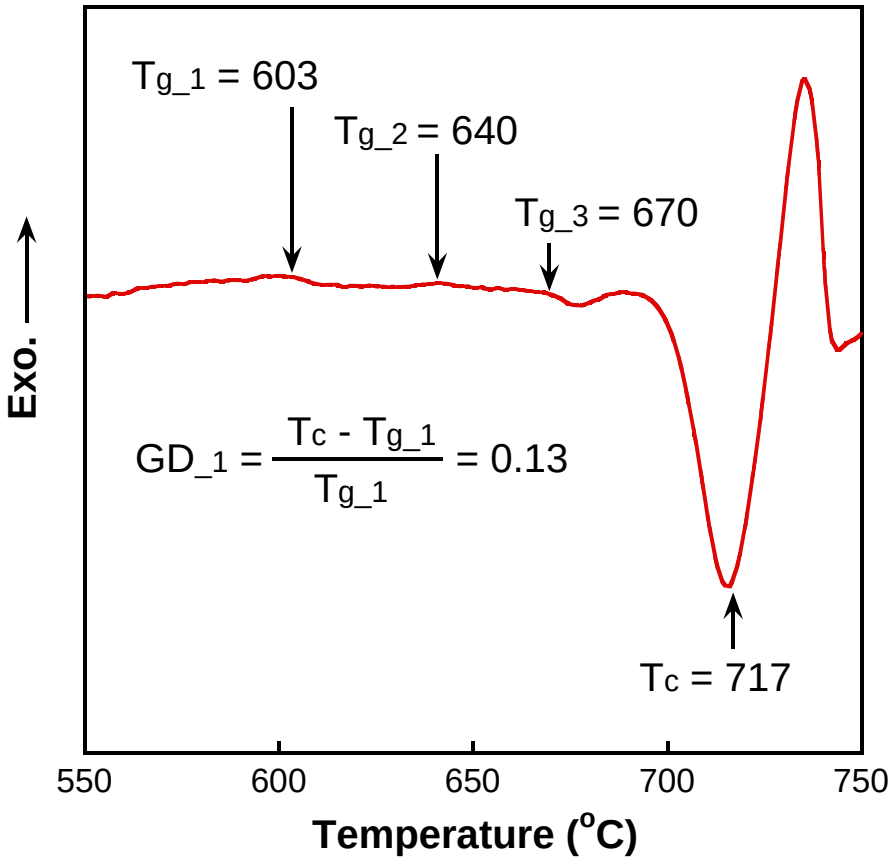

Figure S1: DTA curve of 20P.